

# Dynamic Modeling and Analysis of Omnidirectional Wheeled Robot: Turning Motion Analysis

N.M. Adam<sup>1</sup>, A. Irawan<sup>1</sup>, M. R. Daud<sup>1</sup>, Z. M. Zain<sup>1</sup> and S. N. S. Ali<sup>2</sup>

<sup>1</sup>Robotics and Unmanned Systems (RUS) Research Group, Faculty of Electrical & Electronics Engineering, Universiti Malaysia Pahang.

<sup>2</sup>Vacuumschmelze (M) Sdn. Bhd, Tanah Putih, Lot 3465,26600 Pekan, Pahang, Malaysia. addieirawan@ump.edu.my

**Abstract**—This paper presents the dynamic modeling of a four-mecanum-wheeled mobile robot (4MWMR) to be assessed for frequent turning motion. Overdriven factor in this kind of vehicle motion is one of the issues that need to be tackled for safety and energy efficiencies reasons especially in its turning region. Therefore, this study has taken initiative to analyzing 4MWMR through a structure of mathematical model starting from the inverse kinematics calculation. Moreover, the dynamic model of 4MWMR was calculated using Euler Lagrange approach as a part of the model for torque and force assessment. The analyses are done by using the data history of the experiment of an actual 4MWMR platform as trajectory input to kinematics and dynamics model that connected with 4MWMR transfer function plant. Finally, the performance of 4MWMR parameters; wheel velocity, torque and vehicle axial forces; are demonstrated. From the sample of turning point input, the results show that 4MWMR performing different speed of wheels at different poles during turning session as well as torques. Vehicle longitude force shows the highest since the vehicle is a holonomic system used more force on longitude and latitude axes instead of rotational force on the body.

**Index Terms**—Omnidirectional Wheeled Robot; Mecanum Wheels; Kinematics Model; Dynamic Model; Turning Motion.

## I. INTRODUCTION

Wheeled Mobile Robot (WMR) is one of the mobile robots that attracted a lot of roboticists to enhance its motion control and perception in navigation either remotely control or autonomously. The mobility technologies in the current WMR design makes it suitable for a variety mobile application including for unstructured environment. Fundamentally WMR is classified into three major types as shown in Figure 1; with conventional wheels; with the omnidirectional wheel and with special customized wheels.

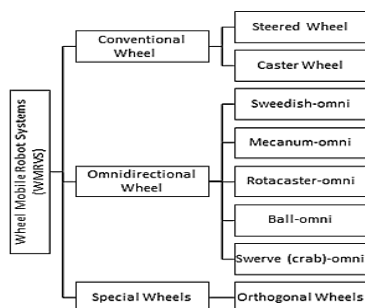


Figure 1: Overview Classifications of Wheeled Mobile Robot Systems (WMRS)

WMR with steered wheels (without offset) and caster wheels are classified under the WMR with a conventional wheel. On the other hand, Sweedish, Mecanum, Rotacaster, Ball, and Swerve are those classified under the Omnidirectional wheel type as shown in Figure 1. These type of Omnidirectional wheel WMR receiving growing attention among the roboticists and various of studies are emphasized on mecanum wheel type with a different number of the wheel such as reported in [1]. The direct and inverse kinematic analysis of four-wheeled omnidirectional WMR with configuration for lateral tilting was done in [2, 3], to demonstrate slip free-motion capability on uneven terrain.

According to the Vicente et al, in order to let the omnidirectional-wheeled vehicle move in a straight line at a specific angle, each wheel must rotate at a specific velocity and direction [4]. Since the mobile robot movement is at angles, trigonometric calculations are necessary so that the wheel speed is determined. Research has been done on how to control the motion planning of the robot by mathematically define the speed of each omnidirectional wheel according to the orientation angle of itself and intended direction by referring [5]. According to the Chang et al., the contribution of each motor consists of the cosine of the angle at the desired direction projected on each wheel drive direction and multiplied the velocities.

According to the [6], the Euler-Lagrange equation was used to producing torque and force (dynamical model) as an element to be controlled in the research. The forces and torque distributions can be calculated from the dynamics model of the omnidirectional mobile robot, from which the control methods can be derived. For example, Wang *et. al.* had proposed allocation-based control with a slacking method for a four-wheeled independent vehicle with the electrical braking system, in which actuator dynamics are taken into consideration [7].

On the other hand, a dynamic control at torque state, as reported in [8], was proposed by analyzing the mathematical relationship between the longitudinal accelerations of wheel's centroid and vehicle in order to be utilized for detecting the tire skid. In [9], the force model of the omnidirectional vehicle control scheme is described. The authors resolved acceleration to design a proportional integral derivative (PID) feedback formula for angular velocity control by a simultaneous stabilization method. In order to determine the body force distribution through the control allocation, the dynamic characteristics of both driving and disturbance are a

model as physical constraints. The simulation is conducted and showed that valid and effective for the system.

This study has taken initiatives to model a 4MWMR system with a combination of kinematic, dynamical and plant model of The Mini Heavy Loaded Forklift Autonomous Guided Vehicle (MHeLFAGV) [10]. This model is designed to assess the performance of the MHeLFAGV system as 4MWMR in terms of speed of each speed and relative to the torques and forces of the system specifically for turning motion. The turning period issues dealt with friction and inertia that may give a different performance for the 4MWMR system. The kinematic model of MHeLFAGV is derived and dynamics of this omnidirectional vehicle are modeled using a Euler-Lagrange method by considering the four mecanum-wheeled individual translation of motion. The paper is organized as follows; Plant modeling of the MHeLFAGV system, Kinematics and Dynamics model for parameter translations, Simulation results, and analysis and wrapped up with the conclusion.

## II. KINEMATIC AND DYNAMIC MODEL OF 4MWMR

As mentioned earlier, the MHeLFAGV system as shown in Figure 2 is a selected 4MWMR model for simulation and analysis. Therefore, the kinematic model of MHeLFAGV was obtained from the fundamental movement and dimension of the vehicle as shown in Figure 2. The parameters of a mecanum wheel reference frame including each roller (internal wheels) mounted on its chassis was notified and relates to a vehicle reference frame via both center of mass (CoM); between  $D$  point for vehicle as shown in Figure 3(a) and  $E$  point for wheel as shown in Figure 3(b). Moreover, the wheel velocity vector is depending on the distance between  $D$ - $E$  points. The axle is mounted normal to the wheel circle as in a standard wheel whereas the contact with the ground is via rollers that are free to spin about an axis in-line with the circle circumference and normal to the wheel axle as shown in Figure 3(b). This enables omnidirectional motion for the vehicle where different velocities of the mecanum wheel are applied.

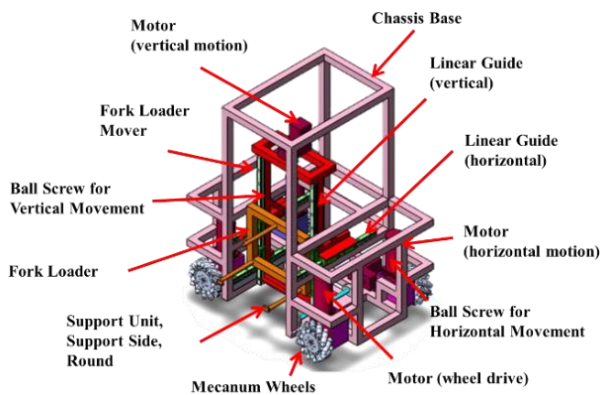


Figure 2: Overview of MHeLFAGV system structure

The key parameters for each roller are  $\alpha$  the angle of ' $E$ ' relative to the  $X_2$  axis,  $\beta$  the angle of the wheel's axis relative to  $E$ , and  $\gamma$  is the angle of the rollers' axis relative to the wheel's plane of rotation (these parameters are varying for each wheel). The angular velocity of the wheel ( $\omega$ ) is defined positively for clockwise (CW) rotation looking outward from the vehicle base. Structure topographies of mecanum wheel

are as follows: the wheel consists of the hub and a serial of free rolling rollers, seen from the axes of the hub, outline of the rollers is partly cover with the theoretical circle of the whole wheel, each roller can rotate around its axes, all rollers have the same angle value ( $45^\circ$ ) [11] as shown in Figure 3(b).

### Nomenclature

$Y_1, X_1$	= coordinate frame (m)
$Y_2, X_2$	= vehicle coordinate (m)
$Y_3, X_3$	= wheel coordinate (m)
$\omega$	= vehicle orientation angle (rad)
$O$	= vehicle frame origin
$\theta$	= orientation angle of the vehicle
$\alpha$	= angle of the vector $D$ and $E$
$r$	= radius of each wheel
$G$	= width between $D$ and $E$
$H$	= height between $D$ and $E$
$\beta$	= angle vector $E$
$D$	= center of the vehicle
$D'$	= subset of the $D$
$E$	= center of the wheel
$l$	= the distance between wheels to x-axis
$\tau_1, \tau_2, \tau_3, \tau_4$	= torque of each wheel (N/m)
$f_1, f_2, f_3, f_4$	= traction force of each wheel (N)
$W_1, W_2, W_3, W_4$	= velocities of each wheel (rad/s)

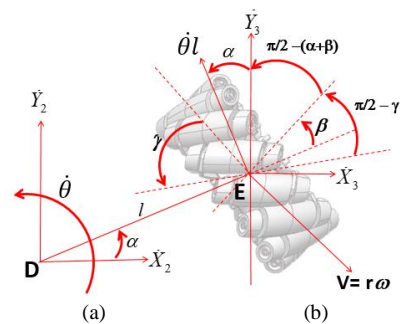


Figure 3: Mecanum wheel coordination and reference frame with respect to MHeLFAGV body frame; (a) reference frame of MHeLFAGV, (b) reference frame of the mecanum wheel

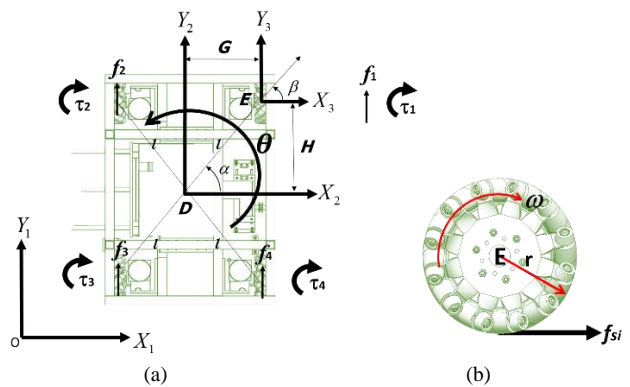


Figure 4: Top view of MHeLFAGV overall system coordination (a) Overall motion and frames, (b) Friction forces in the direction of wheel rotation

The angular differences between the global and local reference frames are given by  $\theta$  [12] and the Cartesian of the vehicle can be expressed as  $q = [\dot{X} \ \dot{Y} \ \dot{\theta}]^T$ . Therefore, with reference to the dimension information in Figure 4 the inverse kinematics (IK) represented by angular velocities of MHeLFAGV's wheels;  $W_1, W_2, W_3,$  and  $W_4$ ; can be calculated and expressed as in Equation (1):

$$\begin{bmatrix} W_1 \\ W_2 \\ W_3 \\ W_4 \end{bmatrix} = \begin{bmatrix} 1 & 1 & l \sin(\frac{\pi}{4}-\alpha) \\ 1 & -1 & l \sin(\frac{\pi}{4}-\alpha) \\ -1 & -1 & l \sin(\frac{\pi}{4}-\alpha) \\ -1 & 1 & l \sin(\frac{\pi}{4}-\alpha) \end{bmatrix} \begin{bmatrix} \cos \theta & \sin \theta & 0 \\ -\sin \theta & \cos \theta & 0 \\ 0 & 0 & 1 \end{bmatrix} \begin{bmatrix} \dot{X}_1 \\ \dot{Y}_1 \\ \dot{\theta} \end{bmatrix} \quad (1)$$

Several studies of the holonomic system [13] have stated that the equations of motion for the type of omnidirectional mobile robot with the mecanum wheel is assumed to be  $\omega=0$  unless some centroid rotating is done which open to another scope of studies. With reference to the Equation (1), the forward kinematic can be expressed as Equation (2);

$$\begin{bmatrix} \dot{X}_1 \\ \dot{Y}_1 \\ \dot{\theta} \end{bmatrix} = J^+ \begin{bmatrix} W_1 \\ W_2 \\ W_3 \\ W_4 \end{bmatrix} \quad (2)$$

where  $J^+=(J^T J)^{-1} J^T$  is the pseudoinverse of  $J$  as shown in Equation (3). In this stage, the objective is to translate the velocity of the MHELFAVGV such that its pose  $q = [\dot{X}_1 \ \dot{Y}_1 \ \dot{\theta}_1]^T$ . follows a reference velocities trajectory  $q = [\dot{X}_D \ \dot{Y}_D \ \dot{\theta}_D]^T$ . Noted that, the first considers a pure translation along a diagonal trajectory in the  $\dot{X}_D \ \dot{Y}_D$  plane with fixed orientation  $\dot{\theta}_D(t) = 0$ .

$$J = \begin{bmatrix} 1 & 1 & l \sin(\frac{\pi}{4}-\alpha) \\ 1 & -1 & l \sin(\frac{\pi}{4}-\alpha) \\ -1 & -1 & l \sin(\frac{\pi}{4}-\alpha) \\ -1 & 1 & l \sin(\frac{\pi}{4}-\alpha) \end{bmatrix} \begin{bmatrix} \cos \theta & \sin \theta & 0 \\ -\sin \theta & \cos \theta & 0 \\ 0 & 0 & 1 \end{bmatrix} \quad (3)$$

In order to determine a comprehensive dynamic analysis of MHELFAVGV, a dynamic model that emphasizes on the mecanum wheel is derived and the coordination of this vehicle dynamic is notified as shown in Figure 4 as well as mecanum wheel coordination. For the case of dynamic model, the resultant forces and torques where the input torques  $\tau = [\tau_1 \ \tau_2 \ \tau_3 \ \tau_4]$  as shown in Figure 4(a) acting on each wheel can be obtained using the expression in Equation (4):

$$\tau_{d_i} = \tau_{c_i} - \tau_{f_i} \quad (4)$$

where  $\tau_{d_i}$  is the torque developed from the difference between current torque of a wheel ( $\tau_{c_i}$ ) and friction torque ( $\tau_{f_i}$ ). The torques can be respectively be calculated using Equations (5) and (6):

$$\tau_{c_i} = m_w W_{o_i} r \quad (5)$$

$$\tau_{f_i} = f_i r \quad (6)$$

where  $m_w$  is the mass of the wheel,  $W_{o_i}$  is the current rotational velocity of the  $i$ -wheel, and  $r$  is the radius of the wheel as shown in Figure 4(b). The torque of  $i$ -wheel ( $\tau_{f_i}$ ) is calculated from forces on each mecanum wheel ( $f_i$ ), which is

considered as the static friction force ( $f_{si}$ ), using the Equation (7):

$$f_{s_i} = \mu(m_b + 4m_w)g \quad (7)$$

where  $m_b$  is the mass of platform in kg,  $g$  is the acceleration due to gravity and  $\mu$  is the coefficient of friction between the mecanum wheel and the road [14]. In general, the friction is classified as static friction, which is a resistance force according to the surface on which the wheel is on the verge of moving [15]. The wheel-road contact forces are critical factors since they present the unique interaction between the vehicle and the surface that it is moving on. Therefore,  $f_i$  in the direction of the wheel rotation must be considered [13], and the frictional force for  $i$ -wheel can be expressed as in Equation (8);

$$f_i = (f_{s_i} \text{sgn}(W_{o_i})) \quad (8)$$

The dynamical model of MHELFAVGV used a Euler-Lagrange approach and the equation can be expressed in Equation (9);

$$\frac{d}{dt} \left( \frac{\partial L}{\partial \dot{q}} \right) - \frac{\partial L}{\partial q} = F_i \quad (9)$$

where  $q_i$  is the  $i^{\text{th}}$  degree of freedom (DoF) variable,  $F_i$  is the external generalized force motion, and  $L$  is the langragian function defined by:

$$L = K - P \quad (10)$$

$K$  is the total kinetic energy including those of the platform and four mecanum wheels and  $P$  is the total potential energy of the vehicle given by:

$$\begin{aligned} K &= T_1 + T_2 + \dots + T_n \\ P &= V_1 + V_2 + \dots + V_n \end{aligned} \quad (11)$$

where  $K_i$  is the of kinetic energy of link (degree of freedom)  $i$ , and  $P_i$  its potential energy. The kinetic energy  $K$  of the vehicle is equal to:

$$K = \frac{1}{2} \left[ m_b + i_b \dot{\theta}^2 + \sum_{i=1}^4 m_w (r_{w_i})^2 + \sum_{i=1}^4 I_i W_i^2 \right] \quad (12)$$

where  $I_b$  is the moment of the inertia of the platform and  $I_i$  is the moment of inertia of each wheel about its main axis,  $r$  is the radius of each mecanum wheel and  $I_i=I, i=1,2,3,4$ . Since the vehicle is assumed moving in a plane, the potential energy  $P=0$ [16]. Then the Euler-Lagrange equations can be a model in terms of kinetic energy. After substituting and some computations, and from the Lagrangian of MHELFAVG system, the Cartesian forces acting on the vehicle can be expressed as in Equation (13) where  $F_{ex} = [F_{X_0} \ F_{Y_0} \ F_{\theta_0}]$  with reference to the CoM of the vehicle as shown in Figure 4(a). Moreover each  $F_{ext}$  expression can be extracted in detail as in Equation (14).

$$\begin{aligned}
 F_{X_0} &= \sum_{i=1}^4 \tau_{d_i} \frac{\partial \dot{W}_o}{\partial X_1}, \\
 F_{Y_0} &= \sum_{i=1}^4 \tau_{c_i} \frac{\partial \dot{W}_o}{\partial Y_1}, \\
 F_{\theta_0} &= \sum_{i=1}^4 \tau_{c_i} \frac{\partial \dot{W}_o}{\partial \theta_1}
 \end{aligned} \tag{13}$$

$$\begin{aligned}
 F_{X_0} &= [\tau_{d_1}] \left[ -\frac{1}{r} (\cos \theta - \sin \theta) \right] + \\
 & [\tau_{d_2}] \left[ -\frac{1}{r} (\cos \theta + \sin \theta) \right] + \\
 & [\tau_{d_3}] \left[ \frac{1}{r} (\cos \theta - \sin \theta) \right] + \\
 & [\tau_{d_4}] \left[ \frac{1}{r} (\cos \theta + \sin \theta) \right] \\
 F_{Y_0} &= [\tau_{c_1}] \left[ -\frac{1}{r} (\sin \theta + \cos \theta) \right] + \\
 & [\tau_{c_2}] \left[ -\frac{1}{r} (\sin \theta - \cos \theta) \right] + \\
 & [\tau_{c_3}] \left[ \frac{1}{r} (\sin \theta + \cos \theta) \right] + \\
 & [\tau_{c_4}] \left[ \frac{1}{r} (\sin \theta - \cos \theta) \right] \\
 F_{\theta_0} &= [\tau_{c_1} + \tau_{c_2} + \tau_{c_3} + \tau_{c_4}] \\
 & \left[ -\frac{\sqrt{2}}{r} l \sin \left( \frac{\pi}{4} - \alpha \right) \right] + \\
 & \left[ \text{sgn } W_{0_1}(f_1) + \text{sgn } W_{0_2}(f_2) + \right. \\
 & \left. \text{sgn } W_{0_3}(f_3) + \text{sgn } W_{0_4}(f_4) \right] \\
 & \left[ -\sqrt{2} l \sin \left( \frac{\pi}{4} - \alpha \right) \right]
 \end{aligned} \tag{14}$$

### III. PLANT ESTABLISHMENT OF 4MWMR

In modeling the MHeLFAGV plant, direct current (DC) brushed motor that used in this vehicle will be used as a plant to be modeled. A DC brushed motor electromechanical system equivalent schematic can be illustrated as shown in in Figure 2 where armature resistance (R) and the armature inductance (L) are the basic components with back emf, ( $e$ ).

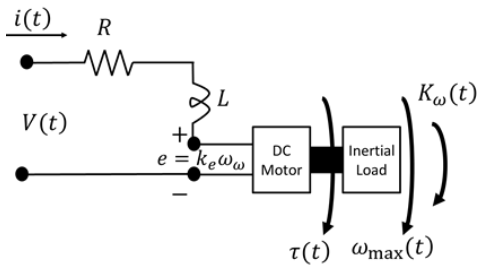


Figure 5: DC motor electromechanical equivalent schematic

Therefore, the mathematical relation for DC brushed motor electromechanical system in Figure 5 can be expressed as Equation (15) and Equation (16);

$$J \frac{d^2 \theta}{dt^2} + b \frac{d\theta}{dt} = ki \tag{15}$$

$$L \frac{di}{dt} + Ri = V - K \frac{d\theta}{dt} \tag{16}$$

where V is the DC source voltage,  $i(t)$  the armature current at time(t), K is armature or emf constant and b is viscous friction. For the case of mechanical properties of the DC brushed motor, the mechanical properties relative to the torque of the system arrangement in Figure 5 would be the product of the inertia of the motor load (J) according to the Newton second law of motion. Then, by using the Laplace transform (LT), Equation (15) and Equation (16) can be expressed as;

$$Js^2 \theta(s) + bs\theta(s) = KI(s) \tag{17}$$

$$Ls(I) + RI(s) = V(s) - Ks\theta(s) \tag{18}$$

where  $s$  is denoting as LT operator, then  $I(s)$  can be expressed as;

$$I(s) = \frac{V(s) - Ks\theta(s)}{R + L(s)} \tag{19}$$

by substitute Equation (19) to the Equation (17), then the equation of the DC brushed motor can be expressed as in Equation (20). From the Equation (20), the transfer function (TF) from the input voltage, V to the output,  $\theta$  can be expressed as in Equation (21).

$$Js^2 \theta(s) + bs\theta(s) = \frac{K(V(s) - Ks\theta(s))}{R + L(s)} \tag{20}$$

$$G(s) = \frac{\theta(s)}{V(s)} = \frac{K}{[s\{(R + sL)(Js + b) + K^2\}]} \tag{21}$$

Table 1  
Parameter Values DC Motor Brush Model Used in MHeLFAGV.

Parameters	Values	Units
L	0.5	H
K	0.01	-
J	0.01	Kg.m <sup>2</sup>
b	0.1	-
R	1	ohm
V <sub>s</sub>	24	V
Stall torque	Nm	174.3
No load current	A	1.68
No load speed (W <sub>max</sub> )	rad/s	13.09
Stall current	A	136.6
Reduction ration	-	24:1

In order to model DC brush motor as a plant modeling and establishment, the parameter values in Table 1 were used. The block diagram for the plant modeling DC brush motor for each wheel then can be modeled. Difference block model is used as a good approximation for error derivative in the discrete model simulation with sample time=1s. A disturbance was added within the model to assessed the response of the system. A slight of the bump will be appearing at 100 seconds due to the disturbance, but the system is able to reject its effect and the steady state error still goes to zero as required. The DC motor brushed model then connected to the angular velocity ( $W_i$ ) that was a model before in inverse kinematic model (IK) in order to get the new velocity ( $W_{oi}$ ) for each wheel. Noted that, the  $W_i$  unit is in rad/s. in order to

connected  $W_i$  and model plant, DC brushed motor, the ratio between wheel speed and voltage input ( $D$ ) is used as Equation (22);

$$D = \left( \frac{W_i}{W_{\max}} \right) V_s \quad (22)$$

where  $W_{\max}$  is the maximum value of speed that produces by DC brushed motor (default manufacturer data). The output of this plant, wheel speed ( $W_{oi}$ ), will be used as an input to the dynamic model in torque and force assessments for each wheel and vehicle respectively.

#### IV. SIMULATION RESULTS AND ANALYSIS

The simulation and analysis are done by using the trajectory waypoint for the X-Y position of the MHeLFAGV experiment as input to the simulation model as shown in Figure 6.

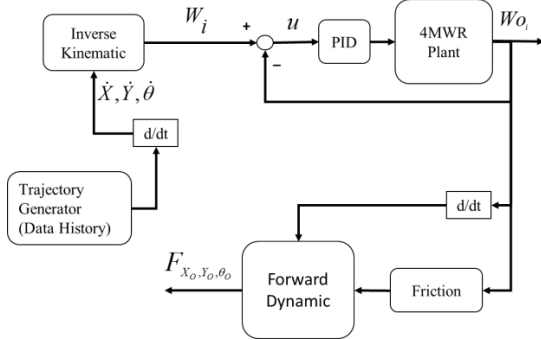


Figure 6: Kinematic and dynamical model structure of MHeLFAGV

In order to assess the performance of MHeLFAGV on turning period, the sample has been taken between two coordination (X-Y position) as shown in Figure 7. A 45-degree quick turning motion like a round shaped experiment data history as shown in Figure 7 was used in this simulation and analysis as trajectory inputs.

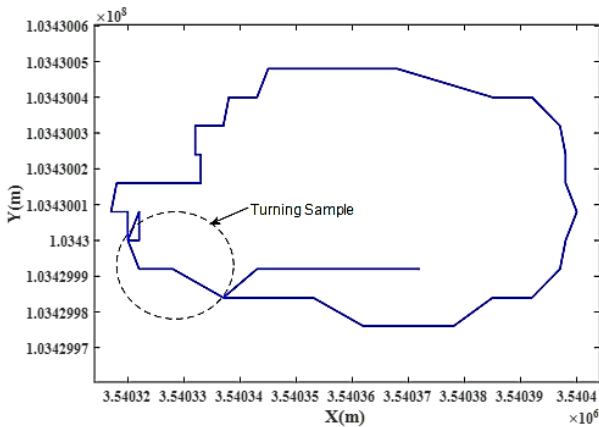


Figure 7: X-Y position of the MHeLFAGV experiment data history used as inputs to the simulation model for turning sample period (10 secs to 20 secs).

As shown in Figure 8, from the sample between 10 secs to 20 secs of simulation time, the rotational velocity of each wheel performed in different values and poles. For example, W1 performed the highest positive speed (forward speed) if

compare to W3 performed the highest negative speed (backward speed) in this period of rotational. This free moves or fully actuated kinematics performed different torque performances as shown in Figure 9 where W4 produced the highest torque and W3 produced the highest reversed torque.

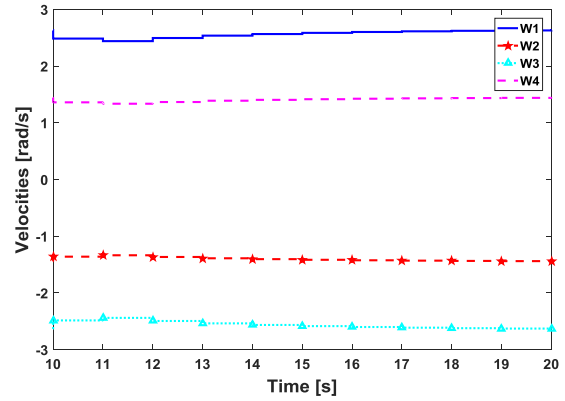


Figure 8: A sample of velocities performance for each wheel after inverse kinematics

It is different to the Cartesian force results as shown in Figure 10, where all forces are assumed to be located at the center of the contact area. First, longitudinal force ( $F_{X_0}$ ) shows the highest at this sample of turning period if compare to the latitude force ( $F_{Y_0}$ ) and vehicle body rotational force ( $F_{\theta_0}$ ) as shown in Figure 10. Moreover  $F_{\theta_0}$  results shows very small force at this moment of period as shown in Figure 10 which is show MHeLFAGV having a very small turning during its turning motion which is unwanted phenomenon for the holonomic system.

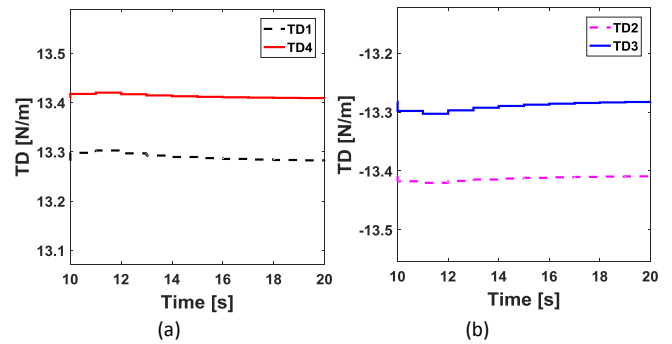


Figure 9: Sample of Developed Torque ( $\tau_D$ ) results for MHeLFAGV system (a)  $\tau_D$  for W1 and W4, (b)  $\tau_D$  for W2 and W3.

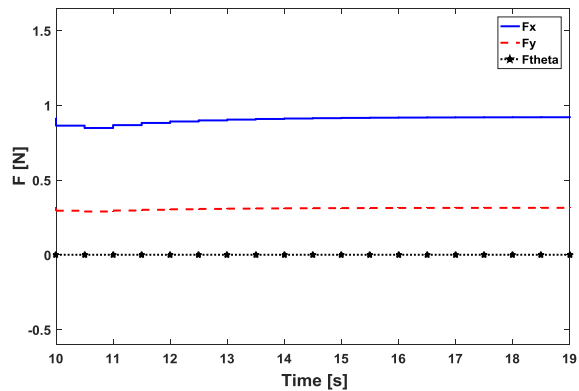


Figure 10: Forces of the MHeLFAGV system (a) longitudinal force ( $F_x$ ), (b) Latitude Force ( $F_y$ ), (c) rotational force ( $F_{\theta}$ )

## V. CONCLUSION

The kinematics and dynamics modeling and analysis of 4MWR according to the MHeLFAGV system is presented. The inverse kinematics able to translate the Cartesian trajectory input of MHeLFAGV to the wheel velocity for plant model inputs. Moreover, the dynamic model of MHeLFAGV via forwarding dynamics able to evaluate the torque for each wheel from plant output as well as calculation the overall vehicle force during movement period. Turning period as a main point of assessment has been done and shows different torques produced by different speed of the wheel. Furthermore, according to a sample of turning period shows the longitude force resulting in the highest force if compare to the other force reaction on the center of the vehicle body. This situation needs a control system that able to consider kinodynamic of the vehicle and it will become a future task for this study.

## ACKNOWLEDGMENT

This research and development is supported by Ministry of Higher Education Malaysia under the Fundamental Research Grant Scheme (FRGS) FRGS/1/2016/TK04/UMP/02/9 (RDU160147) and partially with Universiti Malaysia Pahang (UMP) Research Grant (RDU150348).

## REFERENCES

- [1] M. Sharifi, M. S. Young, X. Chen, D. Clucas, C. Pretty, and W. Meng, "Mechatronic design and development of a non-holonomic omnidirectional mobile robot for automation of primary production," *Cogent Engineering*, vol. 3, p. 1250431, 2016/12/31 2016.
- [2] E. Maulana, M. A. Muslim, and V. Hendrayawan, "Inverse kinematic implementation of four-wheels mecanum drive mobile robot using stepper motors," in *Intelligent Technology and Its Applications (ISITIA), 2015 International Seminar on*, 2015, pp. 51-56.
- [3] K.-L. Han and J. S. Lee, "Iterative Path Tracking of an Omni-Directional Mobile Robot," *Advanced Robotics*, vol. 25, pp. 1817-1838, 2011/01/01 2011.
- [4] A. Vicente, L. Jindong, and Y. Guang-Zhong, "Surface classification based on vibration on omni-wheel mobile base," in *Intelligent Robots and Systems (IROS), 2015 IEEE/RSJ International Conference on*, 2015, pp. 916-921.
- [5] R. Siegwart and I. R. Nourbakhsh, *Introduction to Autonomous Mobile Robots*: Bradford Book, 2004.
- [6] S. Roy and I. N. Kar, "Adaptive-Robust Control of uncertain Euler-Lagrange systems with past data: A time-delayed approach," in *2016 IEEE International Conference on Robotics and Automation (ICRA)*, 2016, pp. 5715-5720.
- [7] Y. Wang, W. Deng, J. Wu, B. Zhu, and S. Zhang, "Allocation-based control for four-wheel independently driven and braked electric vehicle considering actuators' dynamic characteristics," in *2014 IEEE International Conference on Systems, Man, and Cybernetics (SMC)*, 2014, pp. 3354-3359.
- [8] Q. Li, Z. Zhang, and W. Zhao, "Dynamic Control for Four-Wheel Independent Drive Electric Vehicle," in *2012 International Conference on Computer Science and Electronics Engineering*, 2012, pp. 252-256.
- [9] C. C. Tsai, H. L. Wu, F. C. Tai, and Y. S. Chen, "Adaptive backstepping decentralized formation control using fuzzy wavelet neural networks for uncertain mecanum-wheeled omnidirectional multi-vehicles," in *2016 IEEE International Conference on Industrial Technology (ICIT)*, 2016, pp. 1446-1451.
- [10] Norsharimie Adam, Mohd Aiman, Wan Mohd Nafis, Addie Irawan, Mohamad Muaz, Mohamad Hafiz, et al., "Omnidirectional Configuration and Control Approach on Mini Heavy Loaded Forklift Autonomous Guided Vehicle," *MATEC*, 2016.
- [11] W. B. Friedrich Lange, and Michael Suppa, "Force and Trajectory Control of Industrial Robots in Stiff Contact," 2013.
- [12] M. Pena, J. A. Gomez, R. Osorio-Comparan, I. Lopez-Juarez, V. Lomas, H. Gomez, et al., "Fuzzy Logic for Omni directional Mobile Platform Control Displacement using FPGA and Bluetooth," *IEEE Latin America Transactions*, vol. 13, pp. 1907-1914, 2015.
- [13] P. Vlantis, C. P. Bechlioulis, G. Karras, G. Fourlas, and K. J. Kyriakopoulos, "Fault tolerant control for omni-directional mobile platforms with 4 mecanum wheels," in *2016 IEEE International Conference on Robotics and Automation (ICRA)*, 2016, pp. 2395-2400.
- [14] L. Ferriere and B. Raucant, "ROLLMOBS, a new universal wheel concept," in *Proceedings. 1998 IEEE International Conference on Robotics and Automation (Cat. No.98CH36146)*, 1998, pp. 1877-1882 vol.3.
- [15] D. S. Cheon and K. H. Nam, "Steering torque control using variable impedance models for a steer-by-wire system," *International Journal of Automotive Technology*, vol. 18, pp. 263-270, 2017.
- [16] I. J. Cox, T. Lozano-Perez, and G. T. Wilfong, *Autonomous Robot Vehicles*: Springer New York, 2012.